Superstructure and superconductivity in $Li_{1-x}NbO_2$ ($x \approx 0.7$) single crystals

E. G. Moshopoulou,* P. Bordet, and J. J. Capponi
Laboratoire de Cristallographie CNRS–UJF, Boîte Postale 166, 38042 Grenoble, Cedex 09, France
(Received 24 November 1997; revised manuscript received 30 March 1998)

Single-crystal x-ray and electron diffraction studies established a direct relationship between lithium content, crystal structure, niobium valence, and the appearance of superconductivity in the system $Li_{1-x}NbO_2$. The induction of superconductivity by removal of $x \approx 0.3$ lithium is accompanied by the appearance of a superstructure with unit cell $a \times b \times 2c$, where $a \times b \times c$ is the unit cell of the nonsuperconductor $LiNbO_2$. Detailed structural analysis, based on both the main and superlattice reflections, demonstrated that the superconductor $Li_{1-x}NbO_2$ [$x \approx 0.79(9)$, $T_c \approx 5.5$ K] has $P\bar{3}m1$ symmetry, with interlayer ordering of lithium vacancies and weakly distorted [NbO_2] network. As a result of this distortion, Nb cations of the different layers have different valences (3.7^+ and 2.6^+). [S0163-1829(99)10713-6]

I. INTRODUCTION

The system $Li_{1-x}NbO_2$ ($0 \leqslant x \leqslant 0.55$) has received considerable attention since the discovery, by Geselbracht and co-workers,[1] that it exhibits superconductivity ($T_c \approx 5$ K) when $x \approx 0.5$ of lithium is extracted from the nonsuperconducting compound $LiNbO_2$. The reason for this particular attention comes not only from the intrinsic interest of the system itself, but also from the first results reported about this layered, low-T_c superconducting oxide. These results showed that it exhibits certain characteristics that are considered to be typical of the high-T_c cuprates, that is to say (i) elevated density of oxygen states at the Fermi level (E_F) as demonstrated by band-structure calculations,[2] (ii) strongly hybridized $4d$ states of the transition metal (Nb) and $2p$ states of the oxygen at the Fermi level,[2] and (iii) hole type conductivity, as shown by Hall effect measurements.[3] The hope has been that the study of this system and the comparison of its properties with those of the high-T_c copper oxide superconductors could contribute to clarifying the mechanism of the superconductivity in the layered oxides. However, more recent band-structure calculations[4–6] suggested that the nature of superconductivity of $Li_{1-x}NbO_2$ is well described by the BCS model; indeed, according to these studies, the oxygen states definitely appear at E_F, as they do in the high-T_c superconductors, but in the case of $Li_{1-x}NbO_2$ ($x \approx 0.5$) their contribution is much smaller.

The nature of the superconductivity is not the only point of disagreement about this system. Differences in the magnetic behavior of the stoichiometric compound have also been reported. $LiNbO_2$ was found to exhibit temperature-independent paramagnetism with (for single crystals[7,8]) or without (for powders[9]) marked dependence upon magnetic field strength. Band-structure calculations[5,6,10] suggested that $LiNbO_2$ should be diamagnetic, a result confirmed experimentally by Geselbracht and co-workers[11] on powder samples of $LiNbO_2$.

As regards the electronic properties of $LiNbO_2$, band-structure calculations,[5,6,10] optical measurements,[11] and resistivity measurements[9] on compacted powder samples showed that $LiNbO_2$ is a semiconductor. However, the electronic structure of $LiNbO_2$, as calculated by the authors of Ref. 2, suggests that the stoichiometric compound should be metallic or semimetallic.

All the band-structure calculations mentioned above were based on the fact that the crystal structure of the superconducting phase $Li_{1-x}NbO_2$ ($x \approx 0.3$ or $x \approx 0.5$) is identical with that of the nonsuperconducting phase $LiNbO_2$. Indeed, powder x-ray[1,9] diffraction studies showed that the structure of the $LiNbO_2$ (hexagonal symmetry, space group $P6_3/mmc$, $a = 2.9063(6)$ Å, $c = 10.447(2)$ Å, $c/a \approx 3.60$, $Z = 2$) (Refs. 7 and 8) holds for powder samples of $Li_{1-x}NbO_2$ with superconducting volume ≈15%. According to these studies, only the lattice parameters change: $a = 2.9063(6)$ Å, $c = 10.447(2)$ Å in $LiNbO_2$ and $a = 2.919(1)$ Å, $c = 10.453(4)$ Å in $x \approx 0.5$ $Li_{1-x}NbO_2$. Moreover, Kellerman and co-workers,[2] using powder neutron diffraction data, confirmed that a 100% superconducting powder sample of $Li_{1-x}NbO_2$ [$x \approx 0.7$, $a = 2.9275(2)$ Å, $c = 10.4672(9)$ Å] possessed the same crystal structure as that of $LiNbO_2$ [$a = 2.9021(4)$ Å, $c = 10.4500(7)$ Å]. However, no other structural studies have been reported to support these results and to establish that no weak effects (e.g., superstructure, etc.), which could be induced by the decrease of the lithium content, are present in the superconducting phases of the $Li_{1-x}NbO_2$ system.

The correlation between detailed and accurate crystal structure, lithium content, and the appearance of superconductivity is among the key problems to be studied in order to better understand the $Li_{1-x}NbO_2$ system. In this paper we present a thorough investigation[12] of this problem by using single-crystal samples. The use of single crystals is essential for this study; it allows overcoming the problems of the relatively high lithium volatility and of certain dispersion of the lithium content, often present in powder samples of $Li_{1-x}NbO_2$.

II. PREPARATION OF $Li_{1-x}NbO_2$ ($x = 0$, $x \approx 0.3$) SINGLE CRYSTALS AND CHARACTERIZATION OF SAMPLE QUALITY

A. $LiNbO_2$

Single crystals of $LiNbO_2$ were prepared by electrolytic reduction of fused salts. The synthesis method[13] consists

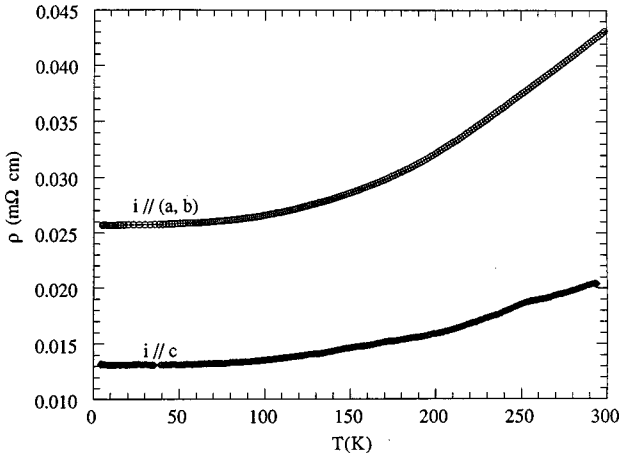

FIG. 1. Resistivity ρ as a function of temperature T for a hexagonal-shaped platelet of $LiNbO_2$ (surface of $2.8\times1.6\,mm^2$ and thickness of 0.2 mm; mass of 121 mg). The data were taken with the current $i=4$ mA parallel to the **c** axis and to the (**a**,**b**) plane, as labeled.

principally of two steps: first, an appropriate oxide is dissolved in a carefully chosen flux and then, electrolysis of this melt, under controlled conditions, produces transition-metal compound(s). For the growth of single crystals of $LiNbO_2$, a mixture of $NaBO_2$, LiF, $LiBO_2$, and Nb_2O_5 has been used. After the electrolysis experiment, red crystals of $LiNbO_2$ were formed on the cathode, and they were separated rapidly from the flux by dissolution in distilled water. The whole synthesis was carried out under argon atmosphere.

The powder x-ray diffraction spectrum of ground crystals was obtained with a Guinier camera with monochromatic Fe $K\alpha$ radiation and using silicon as an internal standard. This spectrum was identical to the previously reported[1,8] spectra of the $LiNbO_2$ and it did not indicate any second phase. Indexing and least-squares refinement of the cell parameters gave $a=2.908(4)$ Å and $c=10.441(2)$ Å, $(c/a=3.591)$; these values are in good agreement with the ones reported in the literature.[1,2,7–9,11,14] The lithium content was determined by atomic absorption spectroscopy (AAS); it was found that the as-prepared crystals (examined immediately after their preparation) were stoichiometric.

In measuring the magnetic susceptibility of $LiNbO_2$ single crystals, we found their magnetic behavior to be very sample dependent. Some single crystals were diamagnetic and others were paramagnetic. Even if no impurities were detected by scanning electron microscopy (SEM) and by powder x-ray diffraction, we cannot conclude anything about the magnetism of $LiNbO_2$, because even the smallest levels of paramagnetic and/or ferromagnetic impurities can modify the intrinsic magnetic response of the sample.

Resistivity measurements were carried out on single crystals of $LiNbO_2$ as a function of the temperature ($T=4-300$ K), in two directions of the current: $i\perp\mathbf{c}$ and $i\|\mathbf{c}$ axis, with $i=4$ mA (Fig. 1). The four electric contacts were made using copper wires attached with silver paint. In opposition to what has previously been predicted[5,6,10] and observed[9,11] on powder samples, $LiNbO_2$ single crystals present semimetallic behavior, with $\rho\,(300\,K)\approx44\,m\Omega\,cm$. This result is consistent with the calculated[2] electronic structure of $LiNbO_2$, according to which the conduction band is almost but not completely filled, suggesting therefore a semimetallic or metallic behavior for the stoichiometric $LiNbO_2$ compound.

TABLE I. Acid solutions used for extraction of lithium from single crystals of $LiNbO_2$, duration t (days) of the chemical treatment and lithium content of the obtained $Li_{1-x}NbO_2$ single crystals. All $LiNbO_2$ crystals were similar in volume and shape (hexagonal platelets of radius $r\approx1.8$ mm and thickness ≈0.6 mm); one crystal was immersed in each solution. The lithium content in each $Li_{1-x}NbO_2$ crystal was determined by measuring (by AAS) the quantity of lithium dissolved in the corresponding solution.

Aqueous solution	Concentration of the solution	Duration t of the treatment (days)	x in $Li_{1-x}NbO_2$
H_2O		14	0.11
HCl	37%	14	0.31
HCl	3% (1 N)	14	0.21
HCl	3% (1 N)	43	0.28
HBr	40%	14	0.12
HNO_3	60%	14	0.16
H_2SO_4	95%	14	0.27
H_3PO_4	85%	14	0.06

B. $Li_{1-x}NbO_2$

Single crystals of $Li_{1-x}NbO_2$ $(x\neq0)$ were prepared by chemical deintercalation of lithium from single crystals of $LiNbO_2$. The choice of the oxidative reagent solution for the deintercalation process and of the reaction conditions (concentration of the solution, duration and temperature of the reaction) was based on the following needs: (i) to conserve the integrity of the single crystals and (ii) to extract controlled quantities of lithium in order to determine the exact x value above which the system $Li_{1-x}NbO_2$ becomes a bulk superconductor. A solution of I_2 or Br_2 in acetonitrile has been successfully used[1–3,9] by several groups to extract lithium from powders of $LiNbO_2$, however when we used it to remove lithium from single crystals of $LiNbO_2$, we could only obtain a powder of mean composition $Li_{0.36}NbO_2$ (determined by AAS). This product presents three superconducting transitions at 2.8, 4.4, and 6.5 K, indicating three phases, probably with at least different lithium contents. It is worth noting here that the composition of the obtained powder, $Li_{0.36}NbO_2$, is the lowest boundary of the lithium content ever reached in this system. In order to avoid the transformation of the single crystals into powders, we used oxidative reagents ''milder'' than acetonitrile: acid aqueous solutions. In Table I, we list the nature and the concentration of the different solutions used and the duration t of the chemical treatment. The chemical treatments were carried out at room temperature (RT). In contrast to the acetonitrile solution, the acid solutions did not destroy the single crystals: their initial geometrical shape was maintained intact as well as their crystallinity (checked on a precession camera). The only modification observed was an alteration in their color; specifically, it changed from red translucent to gray-black, indicating that the electronic properties of the material were modified. From these experiments, it was de-

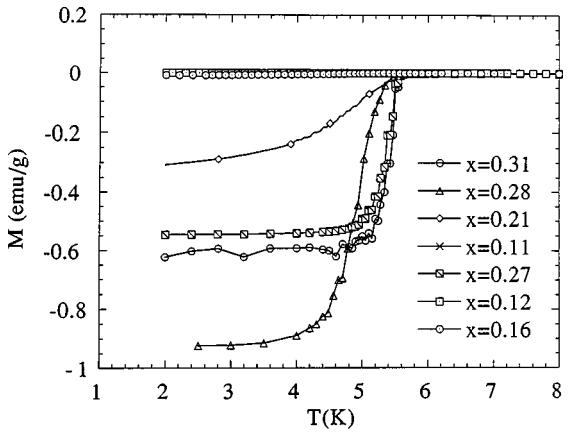

FIG. 2. Zero-field-cooled dc magnetization measurements for single crystals of $Li_{1-x}NbO_2$ for various x as labeled, in an applied magnetic field of 10 Oe parallel to the **c** axis. No correction for demagnetization effects was applied. The solid lines are to guide the eye.

duced that the aqueous HCl solution 1 M, at RT, allows good control of the quantity of lithium to be extracted, by controlling (for crystals of a certain size and shape) the duration t of the chemical treatment. Therefore, for our entire study, we used this solution to prepare the superconducting single crystals of $Li_{1-x}NbO_2$.

As the lithium deintercalation process takes place in a protonic medium, a simple substitution of $H^+ \rightarrow Li^+$ and/or the capture/absorption of H_2O molecules by $Li_{1-x}NbO_2$ might occur. In order to examine this hypothesis, we studied the crystal $Li_{1-x}NbO_2$ with $x \approx 0.28$ (Table I) by Fourier transform infrared spectroscopy. The obtained spectrum does not exhibit the narrow absorption band (3700–3500 cm^{-1}) (Ref. 15) of the stretching vibration of OH^- which would be formed if the protons of the solution substituted the extracted Li^+ cations. Very broad and very weak bands were observed at 3700–3500 and 1630–1600 cm^{-1}; these bands are the absorption bands of stretching vibration of water.[15] Their initial intensity corresponds to traces of water (of the order of ppm) but it increases during the experiment. It was concluded, therefore, that H_2O molecules are not captured from the material during the lithium deintercalation but $Li_{1-x}NbO_2$ ($x \neq 0$, $x = 0$) is humidity-sensitive.

The $Li_{1-x}NbO_2$ ($x \neq 0$) single crystals were characterized by zero-field-cooled (ZFC) and field-cooled (FC) dc magnetization measurements in a field 10 Oe parallel to the **c** axis (Fig. 2). These experiments showed that the superconductivity appears in the $Li_{1-x}NbO_2$ single crystals when the lithium content decreases to ≈ 0.7. This is in agreement with previous results reported[2] on powder samples.

A question of significant importance for our attempt to determine the structure-properties relationship in the $Li_{1-x}NbO_2$ is whether the $Li_{1-x}NbO_2$ single crystals (prepared as described above) present volume superconductivity. Single-crystal x-ray diffraction determines the average crystal structure in the whole volume of the crystal; on the other hand, magnetization measurement gives the diamagnetic behavior and the T_c corresponding at the composition of the surface of a superconducting sample. Therefore, if the composition of the surface is different from that of the volume, any attempt to correlate the appearance of superconductivity with the lithium content and with the corresponding crystal structure in $Li_{1-x}NbO_2$ ($x \neq 0$) single crystals would result in misleading conclusions. A first approach to this question about lithium homogeneity and consequently volume superconductivity in $Li_{1-x}NbO_2$ single crystals involves consideration of the diffusion of lithium ions within the $[NbO_2]$ network. NMR studies[11,16] showed a clear signature of lithium diffusive motion in powders $Li_{1-x}NbO_2$, suggesting therefore an absence of gradients of lithium content in the crystals. These results are consistent with the very high values[2,11,12,14] of the lithium anisotropic Debye-Waller factors of $LiNbO_2$ and $Li_{1-x}NbO_2$. A second piece of evidence that small ($r = 0.1$ mm, thickness $= 0.04$ mm) single crystals $Li_{1-x}NbO_2$ (used for our structural study) were homogeneous in lithium stems from the following structural-chemical consideration: as the evolution of the lattice constants in $Li_{1-x}NbO_2$ ($0 \leqslant x \leqslant 0.3$) depends only on x, any gradient of the lithium content from the surface to the interior of the crystals would result in broader Bragg peaks for the $Li_{1-x}NbO_2$ sample, compared with those of the $LiNbO_2$ sample. We did not observe any significant broadening of the reflections of $Li_{1-x}NbO_2$ compared with the corresponding ones of $LiNbO_2$ during our diffraction experiment (see Sec. IV). Therefore, at least, the small $Li_{1-x}NbO_2$ crystals, used to determine the structure-properties relationship, are bulk superconductors.

III. EVIDENCE OF SUPERSTRUCTURE IN THE SUPERCONDUCTOR $Li_{1-x}NbO_2$ ($x \approx 0.7$)

A. Electron diffraction study of $LiNbO_2$ and $Li_{1-x}NbO_2$ ($x \approx 0.7$)

The aim of the electron diffraction experiments was (i) to investigate eventual static order/disorder effects in $Li_{1-x}NbO_2$, which might result from the decrease of the lithium content, and (ii) to determine whether the Li displacive disorder (suggested by its high Debye-Waller factors) is a true displacive disorder or is due to the presence of an ordered supercell with weak peaks not detected in the x-ray or neutron experiments. For comparison reasons, electron diffraction experiments were also carried out on $LiNbO_2$ single crystals.

Because of the relatively weak bonding between layers in $Li_{1-x}NbO_2$ ($x = 0$, $x \neq 0$), there is strong tendency for crystals to cleave along the (0 0 1) planes. Attempts to prepare TEM specimens only by cleavage did not produce any electron transparent crystallites. Crushing and grinding the crystals in ethanol and recovering of the crystallites from the suspension on a grid produced electron transparent flakelike particles that exhibited a preferred [0 0 1] orientation. It is important to note that these fine crystallites decomposed rapidly (after approximately 1 min) in the presence of oxygen and/or moisture and the crystal structure was destroyed. Their corresponding electron diffraction patterns (taken before electron beam irradiation damage occurs) exhibited amorphous rings passing through very deformed Bragg spots. To avoid this problem, we applied the ''crush and ground'' procedure into a glove box under nitrogen; then the TEM specimen was immediately mounted and transferred to the column of the microscope. The electron diffraction ex-

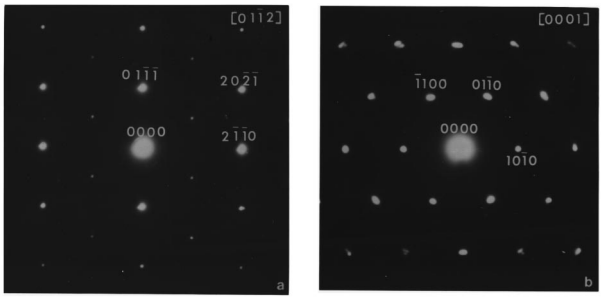

FIG. 3. Selected area diffraction patterns (SAD) of $Li_{1-x}NbO_2$ ($x \approx 0.7$); indexing refers to the hexagonal symmetry of $LiNbO_2$ (space group $P6_3/mmc$, unit cell $a \times b \times c$). (a) $[0\,1\,\bar{1}\,2]$ zone axis pattern showing satellites of type $h\,k\,l/2$ and (b) $[0\,0\,0\,1]$ zone axis pattern, which does not exhibit any superlattice spots. The four-index notation, $h\,k\,i\,l$ with $i=-(h+k)$, is preferable for the indexation of the patterns because it indicates clearly the family of equivalent superstructure reflections.

periments were performed on a Philips EM400 microscope operating at an accelerator voltage of 120 kV.

Preliminary electron diffraction experiments were carried out on several crystallites of both samples in order to examine the stability of the material under the electron beam. It is known that electrons through inelastic scattering process can affect the structure and/or the chemistry of the material. Especially Li compounds are very susceptible to knock-on damage (direct displacement of Li atoms from the crystal lattice) and radiolysis (breaking of the chemical bonds mainly because of heating). Indeed, it was observed that under the 120 kV beam, relatively thick (but still electron transparent) specimens are damaged within 2–3 min. Occasionally, thick specimens were rendered completely amorphous after 4–5 min. Obviously, radiation damage is much more severe and it occurred within much shorter time when convergent beam electron diffraction (CBED) was attempted. Because of this problem we did not try to get any information about the crystal symmetry of $Li_{1-x}NbO_2$ ($x \approx 0.7$) by CBED.

Selected area diffraction (SAD) patterns were taken along the $[0\,0\,1]$, $[2\,\bar{1}\,0]$, $[0\,1\,2]$, $[\bar{2}\,4\,3]$, $[0\,1\,0]$, $[0\,1\,1]$, $[1\,\bar{2}\,\bar{3}]$, etc., zone axis, for several very thin crystallites of both samples. The time of observation of each crystallite was less than 2 min to avoid electron beam irradiation damage. For the $LiNbO_2$ specimen, all diffraction spots could be indexed by using the cell parameters $a = 2.908(4)$ Å and $c = 10.441(2)$ Å obtained from powder x-ray-diffraction data. In the case of $Li_{1-x}NbO_2$ ($x \approx 0.7$), besides the Bragg reflections corresponding to the crystal structure of $LiNbO_2$, the electron diffraction patterns revealed the existence of extra spots at the SAD patterns of the zone axis $[2\,\bar{1}\,0]$, $[0\,1\,0]$, $[1\,\bar{2}\,\bar{3}]$, $[0\,1\,2]$, $[\bar{2}\,4\,3]$, $[0\,1\,1]$. As an example, the pattern along the $[0\,1\,2]$ zone axis is given in Fig. 3(a). Tilting of the specimen $\sim 10°$ about the axis containing the extra spots showed that these spots did not disappear; therefore, they are not due to double diffraction. During these tilting experiments, the intensity of most of the satellites remained stable or decreased slightly for some of them (for example, for $0\,0\,l$ reflections, $l = 2n+1$, in the pattern of zone axis $[2\,\bar{1}\,0]$). In the later case, the double diffraction only contributes to their intensity and is not the main reason for their appearance. Furthermore, a comparison of these experimental patterns with standard spot patterns[17] showed that all the observed extra spots (except $0\,0\,l$ reflections, $l = 2n+1$) appear at positions where no spots are expected due to double diffraction. Therefore, the extra reflections arise from an ordering process probably related to the lithium content in $Li_{1-x}NbO_2$.

Indexing the electron diffraction patterns of $Li_{1-x}NbO_2$ ($x \approx 0.7$), by using the unit cell of $LiNbO_2$ [$a = 2.908(4)$ Å and $c = 10.43(2)$ Å], showed that the superstructure reflections are always of the type $h\,k\,l/2$ ($l = 2n+1$), $h\,h\,l$ ($l = 2n+1$), $0\,0\,l/2$ ($l = 2n+1$). Therefore, more generally, the family of the superstructure reflections is $h\,k\,i\,l/2$, $i = -(h+k)$ with $l = 2n+1$, in the hexagonal four-index notation. The reciprocal plane of the zone axis $[0\,0\,1]$ did not exhibit any evidence of superlattice peaks [Fig. 3(b)]. Therefore, the reciprocal lattice of $Li_{1-x}NbO_2$ ($x \approx 0.7$), defined by the satellites and the main Bragg peaks, is commensurate with the original $LiNbO_2$ reciprocal lattice: all reflections can be indexed using a hexagonal $a \times b \times c'$ supercell, with $c' = 2c$.

Recently, Tyutyunnik *et al.*[18] carried out electron diffraction studies on $Li_{1-x}NbO_2$ ($x \approx 0.59$) (100% superconductor) and $Li_{1-x}NbO_2$ ($x \approx 0.64$) (with superconducting volume 55%) powder samples. This group observed that the SAD patterns of most crystallites of these samples were consistent with the crystal structure of $LiNbO_2$. However, the patterns of some crystallites of $Li_{1-x}NbO_2$ ($x \approx 0.59$) and $Li_{1-x}NbO_2$ ($x \approx 0.64$) present satellites corresponding to $2a \times 2b \times c$ or to $\sqrt{7}a \times \sqrt{7}b \times c$ supercells. We did not observe any of these types of superstructure in the $Li_{1-x}NbO_2$ ($x \approx 0.7$) single crystals.

B. X-ray-diffraction study of $LiNbO_2$ and $Li_{1-x}NbO_2$ ($x \approx 0.7$) on a precession camera

This study was prompted by the following two reasons: first to verify that the superlattice reflections (observed by electron diffraction) are really due to the crystal structure of the superconductor $Li_{1-x}NbO_2$ ($x \approx 0.7$) and they are not induced by the TEM specimen preparation and/or the electron beam; and second to check the quality of the $LiNbO_2$ and $Li_{1-x}NbO_2$ ($x \approx 0.7$) crystals used later (Sec. IV) for the detailed structural investigation.

The sample was a hexagonal platelet of $LiNbO_2$ (hereafter referred to as sample 1), with $r \approx 0.1$ mm and thickness ≈ 0.06 mm. This thickness is very close to the optimum one estimated from the absorption coefficient ($\mu = 246.88\,cm^{-1}$) of $LiNbO_2$ for $\lambda_{Ag\,K\alpha}$ radiation [used later for the detailed structural investigation (see Sec. IV)]. Sample 1 was then transformed to the superconducting $Li_{1-x}NbO_2$ ($x \approx 0.7$) (hereafter referred to as sample 2). The experiments at the precession camera were carried out using acceleration voltage of the x-ray generator $V = 34$ kV in order to eliminate the eventual contribution of a certain, if small, subharmonic $\lambda_{Mo\,K\alpha}/2$, $\lambda_{Mo\,K\alpha}/3$, etc.; these subharmonics could be a source of extra diffracted weak reflections, similar to superlattice reflections. All the experiments were carried out at RT, using Zr-filtered $\lambda_{Mo\,K\alpha} = 0.71$ Å radiation.

Long exposure (≈ 4 days) precession photographs, taken along the $[2\,\bar{1}\,0]$, $[0\,1\,0]$, $[0\,0\,1]$, $[0\,1\,2]$, $[\bar{2}\,4\,3]$, $[0\,1\,1]$

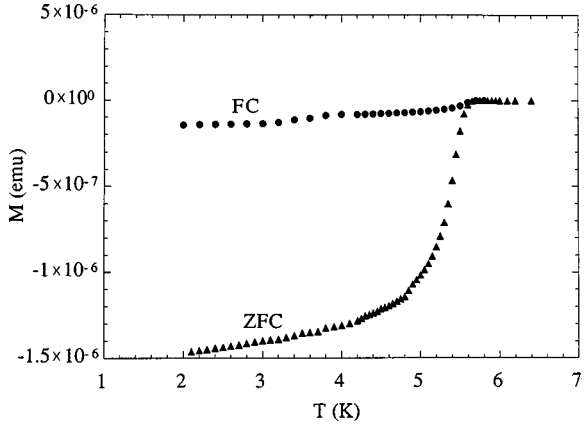

FIG. 4. Zero-field-cooled (▲) and field-cooled (●) dc magnetization measurements for the single crystal of $x \approx 0.79(7)$ $Li_{0.79(7)}NbO_2$ (sample 2) in an applied magnetic field of 10 Oe parallel to the **c** axis, with no correction for demagnetization effects. The Meissner fraction is only ~14% of the shielding fraction; these data suggest that the flux-pinning effects may be strong.

zone axis of the $LiNbO_2$ crystal, did not reveal any superstructure reflections and they were consistent with its known crystal structure.

This crystal was then transformed to $Li_{1-x}NbO_2$ ($x \approx 0.7$) by chemical treatment in HCl 1 N at RT during approximately 310 h. The onset T_c for sample 2 is ≈5.5 K (Fig. 4). Long exposure (≈4 days) precession photos of the $Li_{1-x}NbO_2$ ($x \approx 0.7$) crystal confirmed the existence of the superstructure detected earlier by electron diffraction. No superstructure reflections were observed at the [0 0 1] zone axis pattern.

The observation of the superstructure by x-ray diffraction demonstrates that it is not an artifact of the electron diffraction experiments, but due to a real ordering process related to the lithium content in the sample. Furthermore, as the superstructure appears only in the superconducting phase, it turns out that the induction of superconductivity in this system is related not only to the decrease of the lithium content but also to crystal structure modifications. A clear picture of the structural details related to the superconductivity in $Li_{1-x}NbO_2$ ($x \approx 0.7$) can emerge only by solving the superstructure (based on both the main Bragg peaks and the satellites) and comparing it with the structure of $LiNbO_2$. This study is presented in the next section, which is devoted to the crystal structure investigation of $LiNbO_2$ and $Li_{1-x}NbO_2$ ($x \approx 0.7$).

IV. CRYSTAL STRUCTURE DETERMINATION OF $LiNbO_2$ AND $Li_{1-x}NbO_2$

A. Data acquisition

For the single-crystal x-ray-diffraction data collection (at RT), we used an automatic, computer controlled, four-circle Philips diffractometer, using Ag $K\alpha$ radiation and a graphite monochromator. For both samples 1 and 2, hexagonal cell parameters were refined by the least-squares method using the absolute θ angle of 24 high angle reflections. For $LiNbO_2$: $a = 2.9201(9)$ Å, $c = 10.459(4)$ Å and for $Li_{1-x}NbO_2$ ($x \approx 0.7$): $a = 2.9239(4)$ Å, $c = 10.457(2)$ Å [$c' = 20.914(2)$ Å].

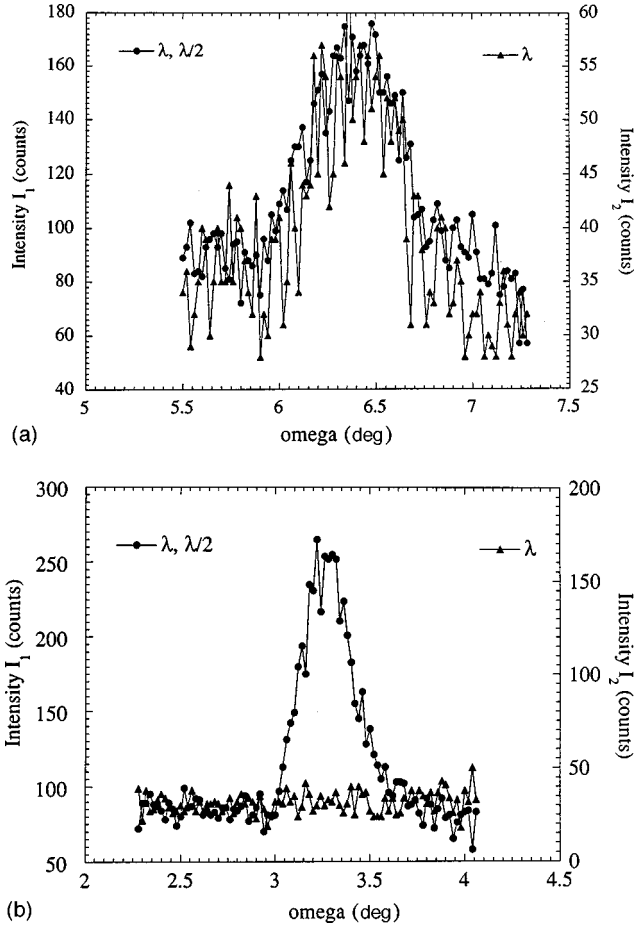

FIG. 5. Reciprocal space intensity profile through the (a) $1\,\bar{1}\,\frac{1}{2}$ and (b) $0\,\frac{2}{2}\,\bar{0}$ reciprocal-lattice points (indexed in the unit cell $a \times b \times c$), from single-crystal x-ray-diffraction data for $x \approx 0.79(7)$ $Li_{1-x}NbO_2$ (sample 2). Closed circles (●) and closed triangles (▲) represent data taken with the contribution of λ and λ/2 and with only the contribution of λ, respectively. The solid lines are to guide the eye. The 2θ angle, where the $1\,\bar{1}\,\frac{1}{2}$ and the $0\,\frac{2}{2}\,0$ would be expected for λ, coincides with the 2θ angle of $1\,\bar{1}\,1$ and 0 2 0, respectively, when λ/2 is used. The data are plotted as a function of the setting angle ω. Because of the bisecting geometry of our experiment, $\omega = \theta$.

The contribution of subharmonic wavelengths (λ/2, λ/3, etc.), mentioned previously for filter-monochromatized radiation, becomes more important when a mosaic monochromator (such as graphite) is used. For this reason, we carried out preliminary ω-2θ scans of several reflections: 0 2 0, 0 0 2, 2 0 3, $1\,\bar{1}\,1$, 1 0 5, $6\,\bar{3}\,12$, 0 0 12, etc., of $LiNbO_2$ and $Li_{1-x}NbO_2$ ($x \approx 0.7$) through their reciprocal space positions 2θ calculated for λ and λ/2. For both samples, before the elimination of λ/2, extra very weak peaks could be detected at the 2θ position of the above reflections corresponding to λ/2. When the subharmonic λ/2 was suppressed, the extra weak reflections at 2θ (corresponding to λ/2) of the main Bragg peaks of both samples were eliminated. However, the superlattice peaks of $Li_{1-x}NbO_2$ ($x \approx 0.7$) were very well detectable even after the suppression of λ/2. Figure 5 shows an example: the $1\,\bar{1}\,\frac{1}{2}$ and the $0\,\frac{2}{2}\,0$ reflections (indexed by the unit cell $a \times b \times c$) of $Li_{1-x}NbO_2$ ($x \approx 0.7$)

TABLE II. Refined structural parameters for $LiNbO_2$ single crystal (sample 1). Space group: $P6_3/mmc$, $Z=2$; unit cell: $a\times b\times c$. Numbers in parentheses are statistical errors of the last significant digit. The expression for the anisotropic temperature factor is $\exp[-2\pi^2(a^{*2}U_{11}h^2+b^{*2}U_{22}k^2+c^{*2}U_{33}l^2+2a^*b^*U_{12}hk+2a^*c^*U_{13}hl+2b^*c^*U_{23}kl)]$. U_{ij} $(i,j=1,2,3)$ are the tensor components of the mean-square amplitude of anisotropic vibration or displacement parameters. By symmetry, for all atoms, $U_{11}=U_{22}=U_{12}$; $U_{13}=U_{23}=0$. The corresponding u_{ij} are the root-mean-square displacement values in Å.

Atom	p	x	y	z	U_{11} (Å^2)	u_{11} (Å)	U_{33} (Å^2)	u_{33} (Å)
Li	0.98(4)	0	0	0	0.032(3)	0.178(8)	0.022(3)	0.15(1)
Nb	1 (fixed)	$\frac{1}{3}$	$\frac{2}{3}$	$\frac{3}{4}$	0.0031(5)	0.056(4)	0.0044(7)	0.066(5)
O	1 (fixed)	$\frac{1}{3}$	$\frac{2}{3}$	0.1285(2)	0.0055(3)	0.074(3)	0.0064(5)	0.080(3)

scanned before (intensity I_1) and after (intensity I_2) the elimination of the $\lambda_{Ag\,K\alpha}/2$ harmonic. These scans are further demonstration (besides the electron diffraction experiments and the study at the precession camera) that the only satellite reflections due to the structure of $Li_{1-x}NbO_2$ $(x\approx 0.7)$ are of the type $h\,k\,l/2$.

For sample 2, $Li_{1-x}NbO_2$ $(x\approx 0.7)$, after the elimination of $\lambda/2$, we verified by ψ scans that the superstructure peaks were not due to multiple diffraction (Renninger effect[19]). In order to choose the appropriate experimental conditions (scan mode, scan speed, reflections' width) that allow correct measurement of their low intensity, ω and ω-2θ scans were carried out on several of them. The superstructure reflections were broader than the principal reflections (indexed by the unit cell $a\times b\times c$) and they were better detectable when scanned in the ω-2θ mode. The broadening of the superstructure peaks reflects the relatively short-range nature of the ordering in our sample. This could be due to the rather high mobility of the lithium ions and/or to small fluctuations of the lithium content in the sample.

For both samples 1 and 2, the data were collected using voltage $V=40$ kV, in order to eliminate the subharmonics $\lambda_{K\alpha\,Ag}/2$, $\lambda_{K\alpha\,Ag}/3$, etc. For sample 1, $LiNbO_2$, the data were collected in the ω-scan mode. For sample 2, $Li_{1-x}NbO_2$ $(x\approx 0.7)$, the intensity measurements were made in the ω-2θ mode; the scan-speed chosen for collecting, in this mode, the weak superstructure reflections was 0.002°/sec. At each experiment, the stability of the beam, of the equipment, and of the crystal was monitored by measuring two standard reflections $0\,1\,\bar{6}$ and $\bar{1}\,1\,0$ at intervals of 60 reflections. The whole sphere in reciprocal space was collected up to $\theta=30°$.

B. Data analysis

1. $LiNbO_2$

The x-ray-diffraction data of sample 1 were corrected for Lorentz-polarization and anisotropic absorption effects (taking into account the dimensions and the shape of the crystal). The intensity and reciprocal space position of the reference reflections showed no significant evolution during the data collection. Then the data were averaged in the point group $6/m$mm. Refinement of the crystal structure was performed taking as an initial model the crystal structure of $LiNbO_2$ as determined by Meyer and Hoppe[7,8] and using the least-squares refinement program MXD.[20] The initial values of the occupancy factors p for all atoms were taken equal to 1. Statistical weights were used and all reflections of positive intensity were included in the refinement. In order to reduce the correlation between parameters, a diagonal block refinement procedure was used, with positional, thermal, and occupancy parameters in separate blocks. Initially, only the scale factor and the z parameter of the oxygen z_O were refined. Then, the atomic displacement parameters U (Å^2), taken isotropic, were varied successively for niobium, oxygen, and lithium atoms. In the next few refinement cycles, anisotropic displacement parameters U_{ij} (Å^2) were introduced and refined with the same sequence; the symmetry restrictions for U_{ij} were obtained from Ref. 21. Then, the lithium occupancy factor was refined together with the z_O and the anisotropic thermal factors of all atoms. Low-angle reflections are known to be generally affected by the effect of the nonspherical contribution of the valence electrons and by the effect of the secondary extinction. Indeed, a comparison between observed and calculated structure factors revealed that strong reflections occurring at low-angle θ values were affected by these effects. Since the number of parameters to be refined was rather small and the number of independent reflections was quite large, the above-mentioned effects were minimized by excluding from the refinements all reflections occurring at low θ angles. Thus, the final refinement cycles were carried out with reflections having $\sin\theta/\lambda>0.2$ with all the parameters varied simultaneously. The obtained R, R_w, and χ^2 were 0.0127, 0.0102, and 0.741, respectively.

The results from the crystal structure analysis of $LiNbO_2$ are given in Table II. They are in good agreement with those reported earlier in the literature.[8,11,14] It is interesting to note that the single-crystal x-ray-diffraction technique allows an accurate and rather precise determination of the lithium content in this compound. In the case of an as-grown crystal, the lithium content is found to be equal to 0.98(4), confirming our previous results obtained by AAS. The strong and quite isotropic thermal vibrations of the Li^+ probably reflect the weakness of the Li-O bonds, related to the easy diffusive motion of Li^+.

2. $Li_{1-x}NbO_2$ $(x\approx 0.7)$

The diffraction data of $Li_{1-x}NbO_2$ were corrected from Lorentz-polarization and anisotropic absorption effects the same way as previously for $LiNbO_2$. The intensity and position of the reference reflections showed no variation during the data collection.

The electron and x-ray-diffraction experiments showed that the main reciprocal lattice of the $Li_{1-x}NbO_2$ $(x\approx 0.7)$is the same as the reciprocal lattice of the $LiNbO_2$. Furthermore, the reciprocal lattice of $Li_{1-x}NbO_2$, defined by the satellites, appears to be commensurate with the original one:

TABLE III. Initial positional model of $Li_{1-x}NbO_2$ ($x \approx 0.7$) (columns 1 and 2) derived from that of $LiNbO_2$ (columns 3 and 4). All the atomic positions (generated by the symmetry) are given.

$P\bar{3}m1$, $(a,b,c'=2c)$, $Z=4$, origin at $\bar{3}m1$		$P6_3/mmc$, (a,b,c), $Z=2$, origin at $\bar{3}m1$	
Li1 at $1\alpha\ \bar{3}m$	(0,0,0)	Li1 at $1\alpha\ \bar{3}m$	(0,0,0)
Li3 at $2c\ 3m$	$(0,0,z)$; $z \approx 0.25$	Li1 at $1\alpha\ \bar{3}m$	(0,0,0.5)
Li2 at $1b\ \bar{3}m$	(0,0,0.5)		
Li3 at $2c\ 3m$	$(0,0,\bar{z})$; $z \approx 0.25$		
Nb2 at $2d\ 3m$	$(\frac{2}{3},\frac{1}{3},\bar{z})$; $z \approx 0.875$	Nb at $2d\ \bar{6}m2$	$(\frac{2}{3},\frac{1}{3},\frac{1}{4})$
Nb1 at $2d\ 3m$	$(\frac{1}{3},\frac{2}{3},z)$; $z \approx 0.375$	Nb at $2d\ \bar{6}m2$	$(\frac{1}{3},\frac{2}{3},\frac{3}{4})$
Nb1 at $2d\ 3m$	$(\frac{2}{3},\frac{1}{3},\bar{z})$; $z \approx 0.375$		
Nb2 at $2d\ 3m$	$(\frac{1}{3},\frac{2}{3},z)$; $z \approx 0.875$		
O1 at $2d\ 3m$	$(\frac{1}{3},\frac{2}{3},z)$; $z \approx 0.064$	O at $4f\ 3m$	$(\frac{1}{3},\frac{2}{3},z)$; $z \approx 0.128$
O3 at $2d\ 3m$	$(\frac{1}{3},\frac{2}{3},z)$; $z \approx 0.186$	O at $4f\ 3m$	$(\frac{1}{3},\frac{2}{3},\frac{1}{2}-z)$; $z \approx 0.128$
O2 at $2d\ 3m$	$(\frac{2}{3},\frac{1}{3},\bar{z})$; $z \approx 0.686$	O at $4f\ 3m$	$(\frac{2}{3},\frac{1}{3},\frac{1}{2}+z)$; $z \approx 0.128$
O4 at $2d\ 3m$	$(\frac{2}{3},\frac{1}{3},\bar{z})$; $z \approx 0.564$	O at $4f\ 3m$	$(\frac{2}{3},\frac{1}{3},\bar{z})$; $z \approx 0.128$
O4 at $2d\ 3m$	$(\frac{1}{3},\frac{2}{3},z)$; $z \approx 0.564$		
O2 at $2d\ 3m$	$(\frac{1}{3},\frac{2}{3},z)$; $z \approx 0.686$		
O3 at $2d\ 3m$	$(\frac{2}{3},\frac{1}{3},\bar{z})$; $z \approx 0.186$		
O1 at $2d\ 3m$	$(\frac{2}{3},\frac{1}{3},\bar{z})$; $z \approx 0.064$		

all observed reflections can be indexed using a primitive $a \times b \times c'$ (where $c'=2c$) supercell. In the cell $a \times b \times c$ of $LiNbO_2$, the 6_3-fold screw axis, which coincides with the **c** axis, applies to each atom (additionally to a rotation of 60°) a translation of $c/2$ parallel to the **c** axis. In the supercell $a \times b \times 2c$ the same translation becomes $c'/4$ ($=c/2$). Therefore, the 6-fold axis can no longer exist in the supercell $a \times b \times c'$, because it does not allow translations $c'/4$. Consequently, the initial hexagonal symmetry has to be lowered at least to trigonal. The choice of the trigonal space group for $Li_{1-x}NbO_2$ is based on the following needs: first, this trigonal space group has to allow the description of the atomic positions in the supercell $a \times b \times c'$, by using the atomic positions in the original hexagonal cell $a \times b \times c$; second, the systematic extinctions of the trigonal space group should be consistent with the diffraction data (main and superlattice reflections) of $Li_{1-x}NbO_2$ ($x \approx 0.7$); and finally, it should have the highest possible symmetry. Among the trigonal space groups,[22] only $P3$, $P\bar{3}$, $P321$, and $P\bar{3}m1$ satisfy all these conditions. It is worth remarking here that because the structures of $Li_{1-x}NbO_2$ ($x \approx 0.7$) and $LiNbO_2$ are strongly connected, their corresponding space groups eventually reflect this connection and therefore the space group of $Li_{1-x}NbO_2$ ($x \approx 0.7$) might be a subgroup of the space group of $LiNbO_2$. Between the above four space groups only $P\bar{3}m1$ is a maximal nonisomorphic subgroup of $P6_3/mmc$.

Initially, analysis of the data and refinements in the space groups $P3$, $P321$, and $P\bar{3}$ were tried. The refinements in the

TABLE IV. Refined structural parameters for $Li_{0.79(7)}NbO_2$ single crystal (sample 2). Space group: $P\bar{3}m1$, $Z=4$; unit cell: $a \times b \times c'$, $c'=2c$. For the $P\bar{3}m1$ space group and for the $1a$, $1b$, $2c$ special positions of Li, $2d$ special positions of Nb, and $2d$ special positions of O, the restrictions on the atomic displacement parameters for all atoms are the following (Ref. 21): $U_{11}=U_{22}=U_{12}$; $U_{13}=U_{23}=0$. The thermal vibration of Li was refined isotropically, therefore $U_{ij}=U_{iso}$.

Atom	p	x	y	z	U_{11} (Å^2)	u_{11} (Å)	U_{33} (Å^2)	u_{33} (Å)
Li1	1 (fixed)	0	0	0	0.022(7)	0.15(2)	$=U_{11}$ (Å^2)	$=u_{11}$ (Å)
Li2	0.50(14)	0	0	$\frac{1}{2}$	0.022(7)	0.15(2)	$=U_{11}$ (Å^2)	$=u_{11}$ (Å)
Li3	0.84(7)	0	0	0.248(6)	0.022(7)	0.15(2)	$=U_{11}$ (Å^2)	$=u_{11}$ (Å)
Nb1	1	$\frac{1}{3}$	$\frac{2}{3}$	0.3741(2)	0.0070(5)	0.084(3)	0.019(2)	0.138(7)
Nb2	1	$\frac{1}{3}$	$\frac{2}{3}$	0.8755(2)	0.0070(5)	0.084(3)	0.019(2)	0.138(7)
O1	1	$\frac{1}{3}$	$\frac{2}{3}$	0.058(1)	0.013(3)	0.114(2)	0.014(7)	0.12(3)
O2	1	$\frac{1}{3}$	$\frac{2}{3}$	0.680(1)	0.013(3)	0.114(2)	0.014(7)	0.12(3)
O3	1	$\frac{1}{3}$	$\frac{2}{3}$	0.188(1)	0.013(3)	0.114(2)	0.014(7)	0.12(3)
O4	1	$\frac{1}{3}$	$\frac{2}{3}$	0.572(1)	0.013(3)	0.114(2)	0.014(7)	0.12(3)

TABLE V. Interatomic distances (Å) and niobium valences for $LiNbO_2$ and $Li_{0.79(7)}NbO_2$.

$LiNbO_2$		$Li_{1-x}NbO_2$ [x≈0.79(7)]	
Li-O×2	2.155(1)	Li1-O1×6	2.074(15)
Li-O×2	2.157(1)	Li2-O4×6	2.264(19)
		Li3-O2×3	2.261(84)
		Li3-O3×3	2.106(75)
Nb-O×4	2.110(1)	Nb1-O2×3	2.034(15)
Nb-O×2	2.114(1)	Nb1-O4×3	2.029(16)
		Nb2-O1×3	2.192(16)
		Nb2-O3×3	2.143(15)
v (Nb)	2.998(8)	v (Nb1)	3.72(16)
		v (Nb2)	2.58(11)

noncentrosymmetric space $P3$, $P321$ diverged, while the refinement in the centrosymmetric space group $P\bar{3}$ yielded at the final cycles a high residual factor: $R=17.49$, $R_w=22.84$, and $\chi^2=8.98$. Attempts to refine the structure by using the space group $P\bar{3}m1$ led to a substantially lower residual index since the first cycles of the refinement. It was concluded therefore that the structure of $Li_{1-x}NbO_2$ ($x\approx0.7$) belongs to the space group $P\bar{3}m1$; thus the details of the data analysis and refinement only within this space group will be given in the next paragraph.

Table III gives the atomic positions for lithium, niobium, and oxygen in the supercell $a\times b\times c'$ with space-group symmetry $P\bar{3}m1$. They are derived from those in the cell $a\times b\times c$ with space-group symmetry $P6_3/mmc$. Therefore, the starting positional model for the refinement of the crystal structure of $Li_{1-x}NbO_2$ ($x\approx0.7$) is given in the second column of Table III. We note that in $Li_{1-x}NbO_2$, the lithium, niobium, and oxygen atoms are split into 3, 2, and 4 crystallographically independent positions, respectively. In the initial structural model, the thermal factors B of all atoms were taken isotropic with starting values equal to those obtained previously from the refinement of the structure of $LiNbO_2$ (Table II). The same types of atoms were constrained to have equal thermal factors. The initial values of the occupancy factors p for all the atoms were taken equal to 1.

The corrected x-ray-diffraction data were averaged in the point group $\bar{3}m$. The structure refinement technique used was the same as that described in Sec. IV B 1 for $LiNbO_2$ and the first refinement cycles were carried out similarly to the corresponding ones for $LiNbO_2$. Then, anisotropic displacement parameters $U_{ij}(Å^2)$ were refined for Nb1, Nb2, and for O1, O2, O3, and O4. For Li1, Li2, and Li3, isotropic thermal factors $U(Å^2)$ were refined because attempts to refine anisotropic ones (required by the symmetry) led to unrealistic results. In the next refinement cycles, besides the scale factor, the positional parameters, and the thermal factors, the occupancy factors of Li1, Li2, and Li3 were also varied. Since the refinement of the occupancy factor of Li1 led to a value slightly above 1, it was subsequently fixed to 1. The occupancy factors of the Nb1, Nb2, and of O1, O2, O3, and O4 were also kept fixed to 1 because attempts to refine them led to values equal to 1 within the experimental precision. For the same reasons as those in the case of $LiNbO_2$ (explained in Sec. IV B 1), the final refinement cycles were carried out only with reflections having $\sin\theta/\lambda>0.2$. In these final refinement cycles the scale factor, seven positional parameters, six thermal factors, and two occupancy factors were varied simultaneously. The obtained R, R_w, and χ^2 were 0.040, 0.0233, and 1.64, respectively. The final fractional atomic coordinates, atomic displacement parameters, and occupancy factors are listed in Table IV. The lists of observed and calculated structure factors are omitted, but are available upon request.

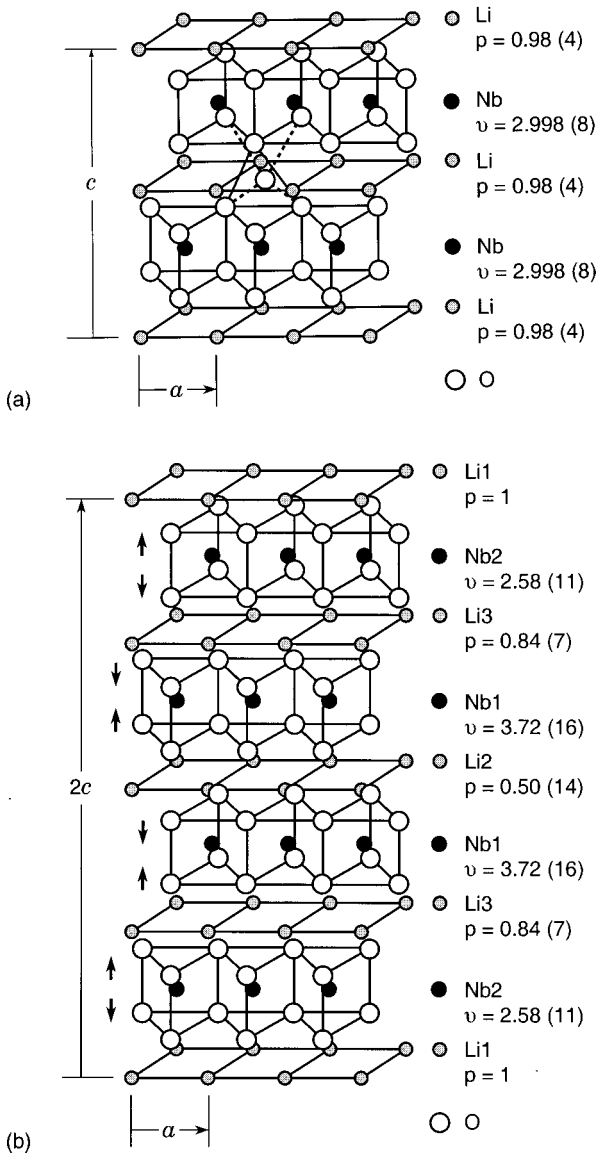

FIG. 6. (a) Schematic of the structure (Ref. 1) of the nonsuperconductor $LiNbO_2$. One row of niobium atoms and two rows of lithium atoms are shown in each of their respective layers. Sufficient oxygen atoms are shown to indicate the trigonal prismatic and the octahedral coordination of the niobium and lithium atoms, respectively. (b) Schematic of the structure of the superconductor $Li_{1-x}NbO_2$ [$x=0.79(7)$]. The two types of distortions of the trigonal prisms of oxygen, at consecutive [NbO_2] layers, are indicated by arrows. The three different lithium occupancies of the octahedral sites between [NbO_2] layers are noted; the valence of Nb at each [NbO_2] layer is also given.

The interatomic distances, calculated using the refined lattice constants and the final positional parameters, are compared for $LiNbO_2$ and $Li_{1-x}NbO_2$ $[x=0.79(7)]$, in Table V. The niobium valences for both compounds were calculated from the empirical formula of Brown-Altermatt[23] using the calculated interatomic distances and the refined occupancy factors of the atoms. The cation-anion constants needed for the valence calculation are taken from Ref. 24. The niobium valences are also compared in Table V.

V. DISCUSSION AND CONCLUDING REMARKS

The crystal structure of the superconducting phase $Li_{1-x}NbO_2$ $[x=0.79(7)]$, as determined from our structural analysis, is shown in Fig. 6(b); for comparison the structure of $LiNbO_2$ is also shown in Fig. 6(a). $LiNbO_2$ can be described[1] as an alternate stacking along the **c** axis of layers of $[LiO_6]$ octahedra and layers of edge-sharing $[NbO_6]$ trigonal prisms. The structure of the superconducting $Li_{1-x}NbO_2$ $[x=0.79(7)]$ consists in a small ordered distortion of the structure of the nonsuperconductor $LiNbO_2$. The results of the refinements indicate that the driving mechanism of this superstructure is the ordering of the lithium vacancies in consecutive layers of $[LiO_6]$ octahedra. Indeed, the lithium occupancy factors for the three nonequivalent positions are $p\_Li1=1.0$ for Li1 at $z=0$; $p\_Li3=0.84(7)$ for Li3 at $z\approx0.25$ and $z\approx0.75$; and $p\_Li2=0.5(1)$ for Li2 at $z=0.5$. The average lithium composition resulting from these lithium occupancy factors is 0.79(7). This interlayer ordering of the lithium vacancies has interesting consequences on the structure of the $[NbO_2]$ network. The niobium and lithium cations almost do not move from their positions in the stoichiometric compound: $z\_Nb1=0.3741(2)$ and $z\_Nb2=0.8755(2)$ in the $a\times b\times c'$ cell of $x\approx0.79(7)$ $Li_{1-x}NbO_2$, compared to $z\_Nb1=0.375$ and $z\_Nb2=0.875$ in a double unit cell $(a\times b\times 2c)$ of $LiNbO_2$; $z\_Li1=0$, $z\_Li2=0.5$, and $z\_Li3=0.248(6)$ in the $a\times b\times c'$ cell $Li_{1-x}NbO_2$ $[x=0.79(7)]$, compared to $z\_Li1=0$, $z\_Li2=0.5$, and $z\_Li3=0.25$ in the $a\times b\times 2c$ cell of $LiNbO_2$. However, the z coordinate of the oxygen anions changes noticeably between $LiNbO_2$ and $Li_{1-x}NbO_2$ $[x=0.79(7)]$: $z\_O1=0.058(1)$, $z\_O2=0.680(1)$, $z\_O3=0.188(1)$, $z\_O4=0.572(1)$ in the $a\times b\times c'$ cell $Li_{1-x}NbO_2$ $[x=0.79(7)]$, compared to $z\_O1\approx0.064$, $z\_O2\approx0.686$ and $z\_O3\approx0.186$, $z\_O4\approx0.564$ in the $a\times b\times 2c$ cell of $LiNbO_2$. The O4 anions, lying close to the half-lithium deficient layer at $z=\frac{1}{2}$, move toward the adjacent niobium layers in order to compensate for the lack of charge created by the vacancies. The effect is opposite, although weaker, for the O1 anions which are close to the full lithium layer at $z=0$. The O2 anions surrounding the lithium layer with 85% occupancy move toward the Nb1 layer. The O3 anions almost do not move.

As a consequence of these oxygen displacements, the Nb-O interatomic distances (Table V) are markedly modified on going from the stoichiometric to the lithium-deficient superconducting compound. For the former the average Nb-O distance is 2.111(1) Å, while for the latter these average distances are 2.03(2) and 2.17(2) Å for Nb1 and Nb2, respectively. These changes in the Nb-O distances induce modifications of the niobium cation valences: from 3^+ in the nonsuperconducting phase, it becomes $3.7(2)^+$ and $2.6(2)^+$ for Nb1 and Nb2, respectively, in the superconducting one. The average $3.2(2)^+$ valence is in agreement with the value $3.21(7)^+$, obtained by applying the rule of electrical neutrality for this crystal and considering its stoichiometry $Li_{1-x}NbO_2$ $[x=0.79(7)]$, determined by the refinement. A very likely hypothesis is that this average increase of the niobium valence is the origin of the metallic behavior and the appearance of superconductivity at low temperatures in this compound. This is consistent with the observed hole type conductivity[2,3] (0.2 holes/mol) for the superconducting phase. However, as this increase of the niobium valence results from the decrease of the Nb2 valence and the more important increase of the Nb1 valence, the existence of two types of charge carriers (electrons in the Nb2 layers and holes in the Nb1 layers) cannot be excluded. Further investigations are required to check this hypothesis.

In conclusion, this study establishes a clear relationship between lithium content, detailed crystal structure, and the appearance of superconductivity in the system $Li_{1-x}NbO_2$. The Nb valence in this system is the most important crystallochemical parameter, similarly to Cu valence for high-T_c oxides. Finally, consideration of the structural details, which differentiate the nonsuperconducting from the superconducting phase, can contribute to clarifying the controversy surrounding a large body of published data about this oxide.

ACKNOWLEDGMENTS

E.G.M. wishes to express her gratitude to Professor M. A. Alario-Franco for introducing her to the study of $Li_{1-x}NbO_2$ by electron diffraction and for helpful conversations. She also thanks Dr. J. L. Tholence and Dr. A. Sulpice for making available their magnetometers and Professor J. Chenavas for fruitful discussions. The work of E.G.M. was supported by the French Ministry of Research and Technology.

*Author to whom correspondence should be addressed. Present address: Brookhaven National Laboratory, Department of Physics, Solid State Physics Group, Bldg. 510B, Upton NY 11973; electronic address: evagelia@bnl.gov

[1] M. J. Geselbracht, T. J. Richardson, and A. M. Stacy, Nature (London) **345**, 324 (1990).

[2] D. G. Kellerman, V. S. Gorshov, A. P. Tyutyunnik, V. G. Zubkov, V. A. Perelyaev, T. V. D'yachkova, N. I. Kadyrova, A. S. Fedyukov, S. A. Turzhevskii, V. A. Gubanov, and G. P. Shveikin, Superconductivity **5**, 2035 (1992).

[3] V. P. Zhokov, V. G. Zubkov, I. V. Nomerovannaya, A. A. Makhnev, N. A. Mushnikov, K. R. Krylov, A. I. Ponomarev, and T. B. Charikova, Superconductivity **6**, 2035 (1993).

[4] V. M. Cherkashenko, M. A. Korotin, V. I. Anisimov, V. V. Shumilov, V. R. Galakhov, D. G. Kellerman, V. G. Zubkov, and E. Z. Kurmanev, Z. Phys. B **93**, 417 (1994).

[5] D. L. Novikov, G. A. Gubanov, V. G. Zubkov, and A. J. Freeman, Phys. Rev. B **49**, 15 830 (1994).

[6] S. A. Turzhevsky, D. L. Novikov, G. A. Gubanov, and A. J. Freeman, Phys. Rev. B **50**, 3200 (1994).

[7] G. Meyer and R. Hoppe, Angew. Chem. **13**, 744 (1974).

[8] G. Meyer and R. Hoppe, J. Less-Common Met. **46**, 55 (1976).

[9] N. Kumada, S. Muramatu, F. Muto, and N. Kinomura, J. Solid State Chem. **73**, 33 (1988).
[10] J. K. Burdett and T. Hughbanks, Inorg. Chem. **24**, 1741 (1985).
[11] M. J. Geselbracht, A. M. Stacy, A. R. Garcia, B. G. Silbernagel, and G. H. Kwei, J. Phys. Chem. **97**, 7102 (1993).
[12] E. G. Moshopoulou, Ph.D. thesis, University Joseph Fourier-Grenoble I, 1995.
[13] M. L. L. Andrieux, Ann. Chim. (Paris) **11-12**, 423 (1929); A. Wold and D. Bellavance, in *Preparative Methods in Solid State Chemistry*, edited by Paul Hagenmuller (Academic, New York, 1972), pp. 279–308.
[14] H. F. Roth, G. Meyer, Z. Hu, and G. Kaindl, Z. Anorg. Allg. Chem. **619**, 1369 (1993).
[15] *Handbook of Chemistry and Physics*, 60th ed. (CRC, Cleveland, OH, 1979), p. F247.
[16] A. F. McDowell, D. M. Snyderman, M. S. Conradi, B. G. Silbernagel, and A. M. Stacy, Phys. Rev. B **50**, 15 764 (1994).
[17] J. W. Edington, *Practical Electron Microscopy in Materials Science* (VanNostrand Reinhold, New York, 1976), pp. 310 and 311.
[18] A. P. Tyutyunnik, V. G. Zubcov, D. G. Kellerman, V. A. Pereliaev, A. E. Kar'kin, and G. Svensson, Eur. J. Solid State Inorg. Chem. **33**, 53 (1996).
[19] M. Renninger, Z. Phys. **106**, 146 (1932).
[20] P. Wolphers, J. Appl. Crystallogr. **47**, 192 (1991).
[21] B. T. M. Willis and A. W. Pryor, *Thermal Vibrations in Crystallography* (Cambridge University Press, New York, 1975), pp. 102–110.
[22] *International Tables for Crystallography* (Kluwer Academic, Norwell, MA, 1995), Vol. A, pp. 480–541 and 590–591.
[23] I. D. Brown and D. Altermatt, Acta Crystallogr., Sect. B: Struct. Sci. **41**, 244 (1985).
[24] N. Brese and M. O'Keeffe, Acta Crystallogr., Sect. B: Struct. Sci. **47**, 192 (1991).